ISSN 2466-2232 (Print)
ISSN 2466-2100 (Online)

A Study on the Microstructure and Mechanical Properties of the Coarse Grain Heat Affected Zone in EH40 Grade High Strength Structural Steels

Seonghoon Jeong*,†, Seunglae Hong*, JunSeok Seo*, Ji-Hee Son*, and Hyung Goun Joo*

*Research & Development (R&D) Center, Hyundai Steel Company, Dangjin-Si, 31719, Korea

†Corresponding author: seonghoonid@gmail.com

(Received July 15, 2022; Revised August 10, 2022; Accepted September 13, 2022)

Abstract

In this paper, the effect of the electro gas arc welding (EGW) process with a heat input of 600 kJ/cm on the microstructural and mechanical characteristics was investigated for two types of EH40 high strength hull structural steels, containing Ti and Nb. The coarse grain heat affected zone (CGHAZ), with a peak temperature of 1450 °C, was simulated for both alloys using a material thermal cycle simulator. Tensile and Charpy impact toughness tests were performed to determine the mechanical properties of the CGHAZ, and microstructural analysis was performed using scanning electron microscopy and transmission electron microscopy. Both alloys exhibited a significant loss of impact toughness because of the welding thermal cycle, causing the formation of a brittle phase and the growth of precipitates. The experimental results indicated that although the addition of Ti and Nb had several benefits on mechanical properties, this might be unsuitable for the EGW process owing to the resulting deterioration in impact toughness.

Key Words: EH40 high strength steel, Electro-gas arc welding, Precipitation, Mechanical properties

1. Introduction

In the recent decades, the importance of energy efficiency has grown with the continuous tightening of environmental regulations pertaining to CO_2 emissions [1-4]. In particular, the shipping industry is facing economic challenges owing to industrial-scale growth and unstable fuel prices. Various efforts have been made to address these challenges, and large container carriers of over 18,000 Twenty-foot Equivalent Unit (TEU), using high strength, ultra-thick high strength structural plates, have been developed to increase operational efficiency and structural safety[5-7]. Lee et al. showed the effect of flux-cored arc welding (FCAW) and the characteristics of residual stresses on ultra-thick plates[8]. An et al. examined brittle crack arresting performance of ultra-thick high strength steel with different welding conditions designed for large container carrier[9]. It was also reported that sufficient crack-arresting performance can be obtained through delicate structural design[10].

With the increasing demand for ultra-thick steel plates, research on welding technology for ultra-thick materials is being actively conducted. Conventionally, FCAW and submerged arc welding (SAW) have been widely employed for fabricating vessels because they offer advantages such as automation and wide applicability[11-14]. However, these welding methods entail degradation of productivity when applied to thick plate welding because of the large number of welding deposits[15]. As an alternative process for them, electro-gas arc welding (EGW) has been considered owing to its high productivity compare to other welding methods. While there are challenges for EGW process such as drastic grain coarsening in the heat affected zone (HAZ) and following degradation of the mechanical characteristics, it has been reported that excellent toughness at low temperature can be obtained with high heat input EGW process in various types of steels[16]. Furthermore, previous study have reported that using inclusion as-

sisted microstructure can be helpful for enhancing HAZ characteristics by forming precipitates and acicular ferrite at elevated temperatures[17]. However, more research is required to determine the influence of precipitation on the coarse grain heat affected zone (CGHAZ) when using EGW, particularly tandem EGW, for joining an ultra-thick plate with a large heat input in the range of 500–600 kJ/cm.

Since we believe that the understanding of the EGW process and its influence on the CGHAZ is crucial for increasing process productivity, this study focuses on the investigation of influence of welding thermal cycle with a heat input of 600 kJ/cm on CGHAZ of EH40 grade high strength structural steel. The HAZ simulation was performed using a metal thermal cycle simulator (MTCS), and the microstructural and mechanical characteristics were comprehensively analyzed.

2. Experimental Procedure

The chemical compositions of the steel plates employed in this study is listed in Table 1. The original ingots were fabricated using a vacuum induction melting furnace and then hot-rolled to a thickness of 20 mm prior to water quenching.

CGHAZ simulation with a peak temperature of 1450 ℃ was carried out using a MTCS, and the specimens for simulation were cut and ground into a rectangular bar-shaped specimens (11 mm × 11 mm × 100 mm). The thermal cycle with a heat input of 600 kJ/cm was calculated using the Rosenthal's heat flow equation[18]. Fig. 1 shows a schematic of the thermal cycle used in the experiment.

For the microstructural analysis, the specimen was polished with a silicon carbide (SiC) paper and a diamond suspension prior to etching with a 2% nitric acid solution at room temperature. Optical and scanning electron microscopy (SIGMA HD, Carl Zeiss, Germany) were used for obtaining microstructural images, while the precipitation analysis was conducted using a transmission electron microscope (Tecnai G2 F20, FEI Company, USA) with samples prepared using a carbon extraction replica technique. All the micrographs collected by the microscopes were analyzed using commercial image processing software.

Table 1 Chemical compositions of the steel plates employed for the experiments

	Fe	C	Si	Mn	P	S	etc.
Steel A	Bal.	0.06 ~ 0.10	0.1 ~ 0.3	1.2 ~ 1.8	~0.02	~0.02	Al, N, Ti
Steel B							Al, N, Ti, Nb

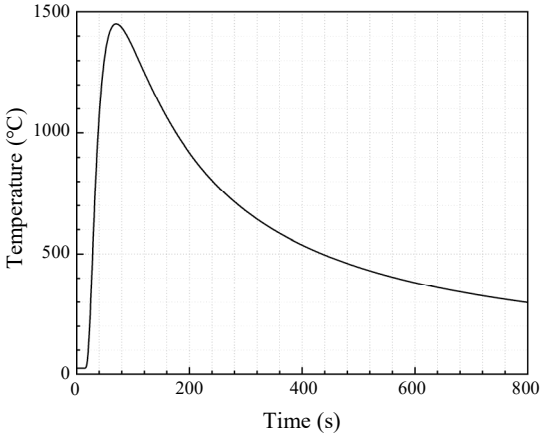

Fig. 1 A schematic of the CGHAZ thermal cycle with a peak temperature of 1450℃

3. Results and Discussion

The mechanical characteristics of the base steels employed in this study and the Charpy impact toughness results of the CGHAZ are listed in Table 2. As shown in the table, both alloys met the international standards of EH40 high strength steel grade, which require a yield strength of over 390 MPa, tensile strength in the range of 510 to 650 MPa, and elongation over 20%. However, the toughness drastically decreased after the CGHAZ simulation regardless of the addition of Nb, while both base steels absorbed over 300 J.

Fig. 2 shows representative microstructure images of

Table 2 Mechanical properties of base steel and CGHAZ in both steels

	Yield strength (MPa)	Tensile strength (MPa)	Elongation (%)	Impact toughness (J)	
				Base steel (-40℃)	CGHAZ (-20℃)
Steel A	409	540	26	332	30
Steel B	428	541	29	356	25

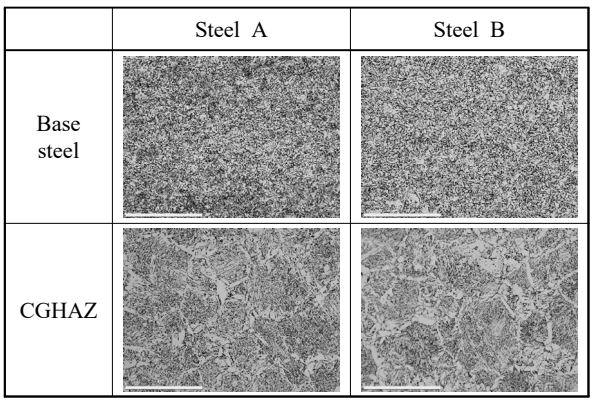

Fig. 2 Representative microstructures of the base steel and CGHAZ in steel A and steel B, obtained by optical microscope

the base steel and CGHAZ. An analysis of these images is required to understand the reason for toughness degradation in the CGHAZ. According to the Fig, steels A and B basically exhibited typical microstructures of high strength C-Mn steels with fine ferrite grains. After the CGHAZ simulation, however, both samples displayed coarsened grains with complex phases composed of grain boundary ferrite, Widmanstätten ferrite, acicular ferrite, and bainitic ferrite. The grain sizes of steel A and steel B were measured as 0.14 μm and 0.15 μm. After the welding thermal cycle, significant coarsening of prior austenite grain (PAG) was observed in each specimen, and the PAG size of steel A and steel B were measured as um 218.8 μm and 264.6 μm. Considering the conditions of weld heat input for the simulated CGHAZ, the grain coarsening behavior was restricted compared to the previous reports[19]. Choi et al. investigated HAZ characteristics in EH36-TM steel with heat input of 342 kJ/cm, having grain size of 348 μm[20]. Kim et al. reported that PAG size can be coarsened up to 800 μm by EGW process with 340 kJ/cm heat input in EH36-TM steel[21]. It is reasonable to say that the presence of Nb and Ti prevented excessive grain coarsening by forming precipitation, which might preserve impact toughness in the CGHAZ[22,23]. However, more discussion should be carried out for detailed understanding the influence of Ti, Nb precipitates, since previous studies have confirmed the side effect of grain refinement in high heat input welding owing to the increasing fraction of grain boundary ferrite, which can have a negative influence on impact toughness[24]. It was also reported that bainitic ferrite may contribute to the toughness drop in the CGHAZ[25,26].

Fig. 3 shows the thermodynamic calculation results for the Ti(C,N) and (Ti,Nb)(C,N) precipitation behavior in both steels, obtained using Thermo-Calc. program. As shown in the Figs, Ti(C,N) in steel A and Ti-dominant (Ti,Nb)(C,N) in steel B had similar dissolution temperatures, while Nb-dominant (Nb,Ti)(C,N) showed a dissolution temperature of 994 °C. It has been reported that the welding thermal cycle can cause abnormal grain coarsening in Ti, Nb added steels because of insufficient pinning and solute drag effect caused by Nb, which explains the larger average grain size of steel B after the CGHAZ simulation[27].

To investigate the effect of precipitation in detail, Fig. 4 shows representative TEM micrographs with the EDS data of particles collected via carbon replica technique for the base steel and CGHAZ in each alloy. As shown in the Figs, nano-sized Ti(C,N) and (Ti,Nb)(C,N) precipitates with rectangular shapes were distributed in both base steels with average particle size of 4.3 nm

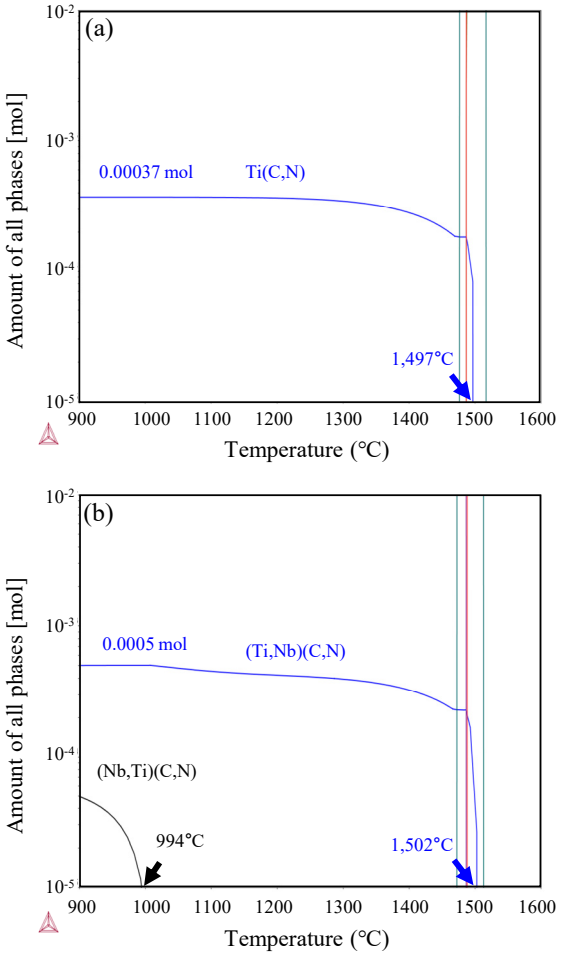

Fig. 3 Thermodynamic calculation results for fraction of precipitation in (a) steel A and (b) steel B

and 3.4 nm, whereas the CGHAZ specimens showed enlarged precipitates with average particle size of 47.9 nm and 89.4 nm. Moon et al. reported that the coarsening behavior of precipitates occurs based on the Gibbs-Thomson effect with critical size, which determines the dissolution of growth behavior[28]. It was well reported that large precipitates can easily cause cleavage fracture by initiating and propagating cracks[29]. As the growth of the particle diameter is directly affected by time at elevated temperatures, it is well accepted that the precipitates in the CGHAZ were coarsened owing to the high welding heat input, causing an extended dwell time at elevated temperature. Moreover, the addition of Nb causes the formation of complex $(Ti_x,Nb_{1-x})(C_y,N_{1-y})$ precipitation with an increased growth rate[30]. Consequently, the pinning effect was reduced in steel B owing to the activated dissolution and growth mechanism of the precipitates.

To understand the specific influence of the precipitates on the mechanical properties of the CGHAZ, representative SEM micrographs of the fracture surfaces for

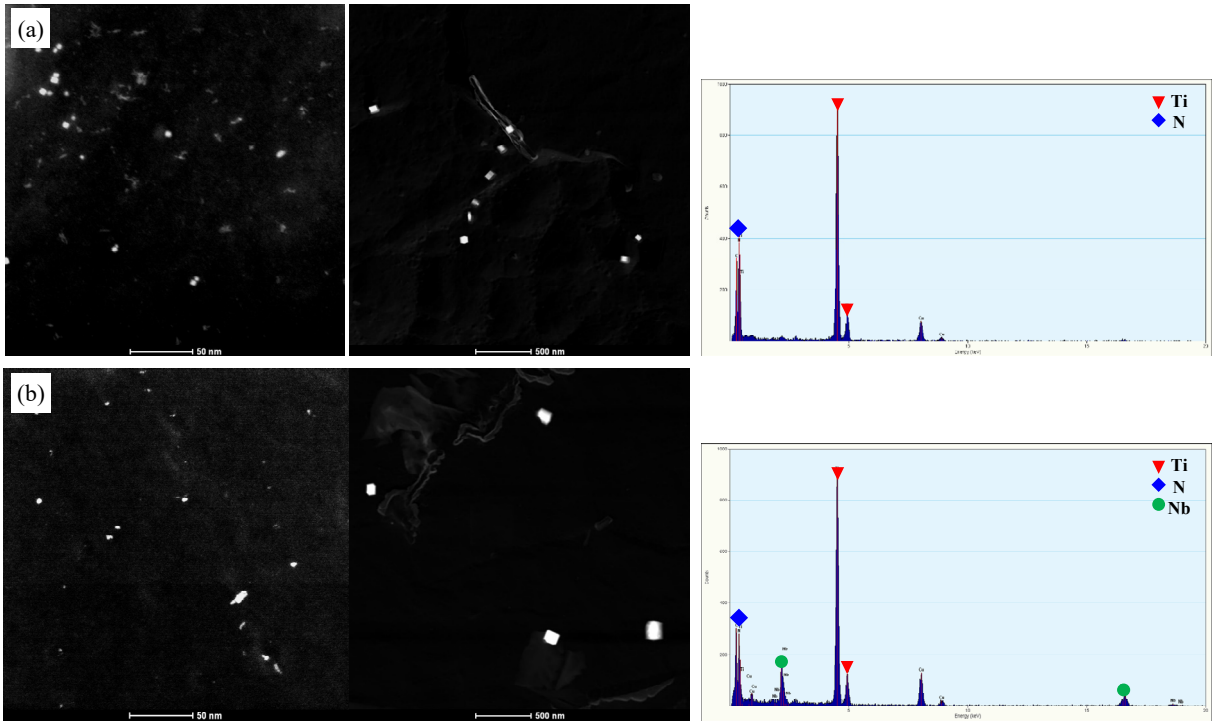

Fig. 4 Representative replica TEM micrographs of base steel and CGHAZ with EDS data in (a) steel A and (b) steel B

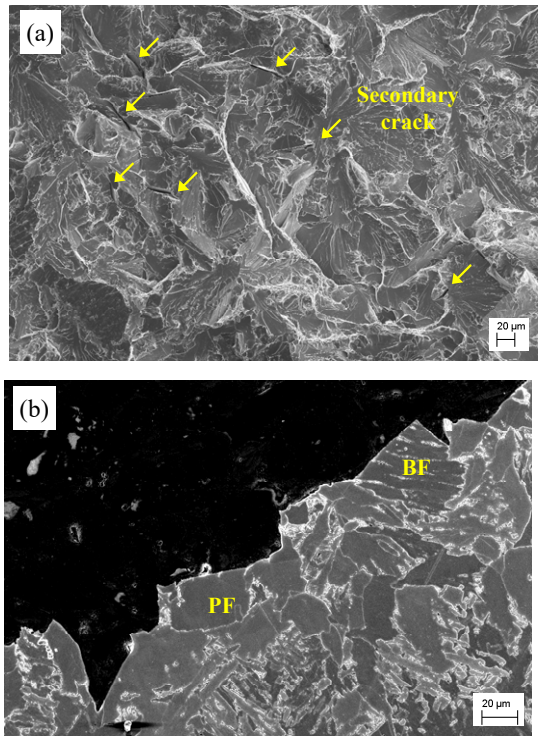

Fig. 5 Fractography showing cleavage fracturing behavior with secondary cracks from (a) top-view and (b) side-view

CGHAZ are shown in Fig. 5. As shown in the Fig, brittle cleavage fracture surface was shown with secondary crack propagation. The crack propagation behavior through ferrite grain boundaries, and bainitic ferrite phase was also observed in the side-view of the fracture surface. By combining the impact toughness results and microstructures, it is conceivable to say that both the presence of precipitation and the formation of brittle phases had a major influence on the mechanical characteristics during the high heat input EGW process by promoting the initiation and propagation of cracks.

Through the comprehensive analyses, we found that high strength steels containing Ti and Nb, which have significant effects on the control of the microstructure and mechanical properties, impart degraded impact toughness to CGHAZ in the EGW process owing to unpredictable growth of precipitation and formation of brittle phases, even if the base steels have excellent mechanical properties. The $(Ti_x, Nb_{1-x})(C_y, N_{1-y})$ precipitates over the critical particle diameter were coarsened during the welding thermal cycle and served as crack initiation sites rather than accelerating acicular ferrite formation and enhancing the pinning effect. Therefore, the results suggest that complex consideration including nitrogen control, precipitation behavior and oxide metallurgy can be a possible and reasonable solution for improving the CGHAZ impact toughness, rather than a single precipitation control. It has been reported that oxide particles can act as a great nucleation sites for acicular ferrite phase[31]. Kang et al. confirmed that nucleation and growth of inclusion has strong influence on microstructure in weld of high strength steel[32]. It

was also demonstrated that Ca, which is a representative oxide former, can inhibit the formation of enlarged TiN precipitates and promote fine particle distribution[33]. As the intra-granular microstructure appears to have a more significant effect on the mechanical characteristics, further studies considering oxide metallurgy should be carried out.

4. Summary

In this study, the microstructure and mechanical properties of the CGHAZ in Ti/Nb-added high strength EH40 grade steels were evaluated under the EGW process with a heat input of 600 kJ/cm. The weld heat thermal cycle was simulated using an MTCS. The following results were obtained.

1) Both Ti and Ti/Nb added steels exhibited a significant reduction in impact toughness in the presence of CGHAZ, and mixed microstructures with bainitic ferrite, Widmanstätten ferrite, and acicular ferrite were observed.

2) According to the Thermo-Calc. calculation and microstructural observation, the steel sample with Ti/Nb had a larger CGHAZ grain size compared to the alloy with Ti because the precipitates dissolved at a relatively low temperature.

3) Microstructural analysis confirmed that the CGHAZ simulation caused the formation of enlarged precipitates and brittle phases, resulting in a drastic reduction in impact toughness.

Acknowledgement

This work has been studied by the research and development centers of the Hyundai Steel Company of the Republic of Korea.

ORCID: Seonghoon Jeong: http://orcid.org/0000-0001-5527-4584

References

1. Y Xing, H Yang, X Ma, and Y Zhang, Optimization of ship speed and fleet deployment under carbon emissions policies for container shipping, *Transport,* 34(2) (2019) 260-274. https://doi.org/10.3846/transport.2019.9317
2. H Xing, S. Spence, and H. Chen, A comprehensive review on countermeasures for CO_2 emissions from ships, *Renew. Sustain. Energy Rev.* 134 (2020) 110222. https://doi.org/10.1016/j.rser.2020.110222
3. G. Park, S. Jeong, and C. Lee, Fusion weldabilities of advanced high manganese steels: A review, *Met. Mater. Int.*27 (7) (2021) 2046-2058. https://doi.org/10.1007/s12540-020-00706-9
4. S. Jeong, S. Hong, J. S. Seo, and W. Choi, Effect of line-heating on the microstructural and mechanical characteristics of 320-MPa-Grade high-strength hull plates, *J. Weld. Join.* 40(4) (2022) 352-357. https://doi.org/10.5781/JWJ.2022.40.4.8
5. A. K. Prokopowicz and J. Andreassen, An evaluation of current trends in container shipping industry, very large container ships (VLCSs), and port capacities to accommodate TTIP increased trade, *Transp. Res. Proc.* 14 (2016) 2910-2919. https://doi.org/10.1016/j.trpro.2016.05.409
6. H. I. Im, N. Vladimir, Š Malenica, and D. S. Cho, Hydroelastic response of 19,000 TEU class ultra large container ship with novel mobile deckhouse for maximizing cargo capacity, *Int. J. Nav. Archit. Ocean Eng.* 9(3) (2017) 339-349. https://doi.org/10.1016/j.ijnaoe.2016.11.004
7. J. Ge, M. Zhu, T. Notteboom, W. Shi, and X. Wan, Towards 25,000 TEU vessels? A comparative economic analysis of ultra-large containership sizes under different market and operational conditions, *Marit. Economics Logist.* 23(4) (2021) 587-614. https://doi.org/10.1057/s41278-019-00136-4
8. J. H. Lee, S. Y. Hwang, Y. S. Yang, and B. J. Kim, Residual stress analysis of multi-layer flux core arc welding in the joint of ultra thick plates, *The Twentieth International Offshore and Polar Engineering Conference, OnePetro* (2010).
9. G. B. An and J. S. Park, Brittle crack arrestability of thick steel plate welds in large structure, *Met. Mater. Int.* 17(5) (2011) 841-845. https://doi.org/10.1007/s12540-011-1023-1
10. E. Tamura, T. Nakagawa, K. Tsutsumi, and N. Furukawa, Effect of steel toughness on brittle crack arrest behavior of T-weld joint structure using thick plates, *Kobelco Technol. Rev.* 30 (2011).
11. J. E. R. Dhas and S. Kumanan, Optimization of parameters of submerged arc weld using non conventional techniques, *Appl. Soft Comput.* 11(8) (2011) 5198-5204. https://doi.org/10.1016/j.asoc.2011.05.041
12. D. Katherasan, J. V. Elias, P. Sathiya, and A. N. Haq, Simulation and parameter optimization of flux cored arc welding using artificial neural network and particle swarm optimization algorithm, *J. Intell. Manuf.* 25(1) (2014) 67-76. https://doi.org/10.1007/s10845-012-0675-0
13. C. Jin and S. Rhee, Real-time weld gap monitoring and quality control algorithm during weaving flux-cored arc welding using deep learning, *Metals,* 11(7) (2021) 1135. https://doi.org/10.3390/met11071135
14. S. S. Sarkar, A. Das, S. Paul, K. Mali, A. Ghosh, R Sarkar, and A. Kumar, Machine learning method to predict and analyse transient temperature in submerged arc welding, *Measurement,* 170 (2021) 108713.

https://doi.org/10.1016/j.measurement.2020.108713
15. D. S. Kim, Welding techniques and welding consumables for shipbuilding and offshore fabrication, *Proceedings of the Welding Metallurgy Symposium of KWJS,* (2008).
16. KM Ryu, DW Kim, JW Lee, HC Bang, CG Park, and H Jeong, High Heat Input Electro-gas Arc Welding of TMCP Plate for Steel Storage Tanks, *J. Weld. Join.* 35(6) (2017) 27-31. https://doi.org/10.5781/JWJ.2017.35.6.5
17. T. Koseki, A review on inclusion-assisted microstructure control in C-Mn and low-alloy steel welds, *Weld. World*, 49(5) (2005) 22-28. https://doi.org/10.1007/BF03263406
18. S. Kou, and Sindo, Welding metallurgy, *New Jersey, USA.* 431(446) (2003) 223-225.
19. H. C. Jeong, Y. H. Park, Y. H. An, and J. B. Lee, Mechanical properties and microstructures of high heat input welded tandem EGW joint in EH36-TM steel, *J. Korean Weld. Join. Soc.* 25(1) (2007) 57-62. https://doi.org/10.5781/KWJS.2007.25.1.057
20. W. H Choi, S. K. Cho, W. K. Choi, S. G. Ko, and J. M. Han, Effects of microstructures on the toughness of high heat input EG welded joint of EH36-TM steel, *J. Korean Weld. Join. Soc.* 30(1) (2012) 64-71. https://doi.org/10.5781/KWJS.2012.30.1.64
21. K. Kim, K. Kim, H. Sim, K. Bae, H. Hong, and B. Park, Effect of groove conditions on the mechanical properties of welds produced by the combined welding process of flux cored arc and electro gas in EH36 TMCP steel plate for hull structures, *J. Weld. Join.* 33(5) (2015) 35-40. https://doi.org/10.5781/JWJ.2015.33.5.35
22. J. Moon and C. Lee, Behavior of (Ti, Nb)(C, N) complex particle during thermomechanical cycling in the weld CGHAZ of a microalloyed steel, *Acta Mater.* 57(7) (2009) 2311-2320. https://doi.org/10.1016/j.actamat.2009.01.042
23. X. Ma, X. Li, B. Langelier, B. Gault, S. Subramanian, and L. Collins, Effects of carbon variation on microstructure evolution in weld heat-affected zone of Nb-Ti microalloyed steels, *Metall. Mater. Trans.* A 49(10) (2018) 4824-4837. https://doi.org/10.1007/s11661-018-4751-8
24. K. Seo, H. Ryoo, H. J. Kim, C. Park, and C. Lee, Local variation of impact toughness in tandem electro-gas welded joint, *Weld. World,* 64(3) (2020) 457-465. https://doi.org/10.1007/s40194-019-00844-800
25. G. Krauss and S. W. Thompson, Ferritic microstructures in continuously cooled low-and ultralow-carbon steels, *ISIJ Int.* 35(8) (1995) 937-945. https://doi.org/10.2355/isijinternational.35.937
26. H. Lee, S. Cho, W. Choi, Y. Kim, Y. Kwon, J. Lee, S. Shin, and D. Choi, Correlation between HAZ microstructure and low temperature impact toughness of bainitic steel plates, *J. Weld. Join.* 39(3) (2021) 269-277. https://doi.org/10.5781/JWJ.2021.39.3.5
27. Y. Yang, X. Jia, Y. Ma, P. Wang, F. Zhu, H. Yang, C. Wang, and S. Wang, Effect of Nb on microstructure and mechanical properties between base metal and high heat input coarse-grain HAZ in a Ti-deoxidized low carbon high strength steel, *J. Mater. Res. Technol.* 18 (2022) 2399-2412. https://doi.org/10.1016/j.jmrt.2022.03.150
28. J Moon, S Kim, J Lee, and C Lee, Coarsening behavior of the (Ti, Nb)(C, N) complex particle in a microalloyed steel weld heat-affected zone considering the critical particle size, *Metall. Mater. Trans.* A 38(11) (2007) 2788-2795. https://doi.org/10.1007/s11661-007-9317-0
29. T. Liu, M. Long, D. Chen, H. Duan, L. Gui, S. Yu, J. Cao, H. Chen, and H. Fan, Effect of coarse TiN inclusions and microstructure on impact toughness fluctuation in Ti micro-alloyed steel, *Res. Int.* 25(10) (2018) 1043-1053. https://doi.org/10.1007/s42243-018-0149-5
30. J. O. Moon and C. H. Lee, Precipitation and precipitate coarsening behavior according to Nb addition in the weld HAZ of a Ti-containing steel, *J. Korean Weld. Join. Soc.* 26(1) (2008) 76-82. https://doi.org/10.5781/KWJS.2008.26.1.076
31. M. Shi, P. Zhang, and F. Zhu, Toughness and microstructure of coarse grain heat affected zone with high heat input welding in Zr-bearing low carbon steel, *ISIJ Int.* 54(1) (2014) 188-192. https://doi.org/10.2355/isijinternational.54.188
32. Y. Kang, S. Jeong, J. H. Kang, and C. Lee, Factors affecting the inclusion potency for acicular ferrite nucleation in high-strength steel welds, *Metall. Mater. Trans.* A 47(6) (2016) 2842-2854. https://doi.org/10.1007/s11661-016-3456-0
33. T. Kato, S. Sato, H. Ohta, and T. Shiwaku, Effects of Ca addition on formation behavior of TiN particles and HAZ toughness in large-heat-input welding, *Kobelco Technol. Rev.* 30 (2011) 76-79.